Available online at www.sciencedirect.com
ScienceDirect
Journal of Fluorine Chemistry 128 (2007) 958–964
JOURNAL OF FLUORINE CHEMISTRY
www.elsevier.com/locate/fluor

Preparation of COF_2 using CO_2 and F_2 in the electrochemical cell with $PbSnF_4$ as a solid electrolyte

Yasuo Hasegawa [b], Akitomo Nagasaka, Kim Jae-Ho, Susumu Yonezawa *, Masayuki Takashima [a]

[a] *Department of Materials Science and Engineering, Faculty of Engineering, Fukui University, 3-9-1 Bunkyo, Fukui 910-8507, Japan*
[b] *Forensic Science Laboratory, Fukui Prefectural Police Headquarters, 3-17-1 Ote, Fukui 910-8515, Japan*

Received 26 February 2007; received in revised form 11 April 2007; accepted 12 April 2007
Available online 18 April 2007

This paper is dedicated to Prof. Neil Bartlett on the occasion of his 75th birthday.

Abstract

Tetragonal $PbSnF_4$ was prepared by precipitation method with $Pb(NO_3)_2$ and SnF_2 aqueous solutions. The product was characterized using X-ray diffraction (XRD), X-ray fluorescence spectroscopy (XFS), and the other chemical analyses. Tetragonal $PbSnF_4$ exhibited the highest electric conductivity of 3.2 Sm^{-1} at 473 K in air as a fluoride ion conductor. We have investigated the possibility of COF_2 formation using CO_2 and F_2 in an electrochemical cell with $PbSnF_4$ as a solid electrolyte. At same time, we tried to produce an electric power from an electrochemical cell. This CO_2/F_2 electrochemical cell was constructed with a tetragonal $PbSnF_4$ disk having Au electrodes. The electromotive force was about 0.9 V at room temperature for 0.1 MPa CO_2/(0.01 MPa F_2 + 0.09 MPa Ar). However, the short circuit current density was 0.24 A m^{-2}, which was quite small. This current density was so small that no fluorocarbon compound was detected after 3 h discharge using FT-IR.

Keywords: COF_2; Electrochemical preparation; Solid electrolyte; Tetragonal $PbSnF_4$

1. Introduction

On the earth each year, 12,100 million tonnes of CO_2 are emitted to the air [1]. The increase of its concentration in the air is causing global warming. Numerous efforts have been made to remove CO_2 from the air. Normally, new methods to reduce CO_2 to CH_3OH and CH_4 have been investigated [2,3]. These investigations are based on the concept that CO_2 is a final product of hydrocarbon compounds' combustion.

A strong oxidant, F_2, can oxidize the oxides. Previously, we reported a reaction between CO_2 and F_2 to form COF_2 [4]. By this reaction, CO_2 can be converted to COF_2. The Gibbs free energy change of this reaction is calculated as 220 kJ mol^{-1} [5]:

$$CO_2 + F_2 \rightarrow COF_2 + \tfrac{1}{2}O_2 + (-\Delta G)\,220\,\mathrm{kJ\,mol^{-1}}$$

Furthermore, the theoretical electromotive force calculated from its Gibbs free energy is 1.14 V, which value is mostly equal to the electromotive force 1.23 V of the H_2/O_2 fuel cell [6]. Based on this idea, we tried to investigate COF_2 formation using CO_2 and F_2 in the electrochemical cell with $PbSnF_4$.

By using the electrochemical cell with solid electrolyte to prepare COF_2, the reaction between CO_2 and F_2 might be controlled by external current flow and the separation of COF_2 from CO_2/F_2 mixture gas is not needed.

Tetragonal $PbSnF_4$ [7–22] is known as a fluoride ion conductor having high electric conductivity at ambient temperatures. $PbSnF_4$ can exist in several polymorphic forms as described by many reports [7,8,14–16], and has a very complex system of phase transitions.

* Corresponding author at: Department of Materials Science and Engineering, Faculty of Engineering, Fukui University, 3-9-1 Bunkyo, Fukui 910-8507, Japan.
E-mail address: yonezawa@matse.fukui-u.ac.jp (S. Yonezawa).

0022-1139/$ – see front matter © 2007 Elsevier B.V. All rights reserved.
doi:10.1016/j.jfluchem.2007.04.016

The CO_2/F_2 electrochemical cell was constructed using tetragonal $PbSnF_4$ as a solid electrolyte and its performance was investigated in detail.

2. Results and discussion

2.1. Preparation of $PbSnF_4$

A synthesis on the MF_2–SnF_2 systems in both aqueous and molten states was carried out by Donaldson and Senior [7]. There are two known main routes to prepare $PbSnF_4$ from solution and by direct reaction at high temperature [7–12].

White sediment was prepared by mixing a $Pb(NO_3)_2$ aqueous solution and SnF_2 solution. The dropping speed was 10 or 500 $mm^3\ s^{-1}$. The hold time after mixing two solutions was 0–24 h. The (0 0 ℓ) peak of tetragonal $PbSnF_4$ became larger with increasing hold time after mixing. It was suitable to prepare tetragonal $PbSnF_4$ at dropping speed 500 $mm^3\ s^{-1}$ further than dropping speed 10 $mm^3\ s^{-1}$. Fig. 1 shows the XRD results of the synthesized sample at various temperatures at a dropping speed 500 $mm^3\ s^{-1}$. The Miller indices are shown in Fig. 1. Compared with Fig. 1(d) referred from the literature [11,22,23], a new peak was observed at $2\theta = 6.9^\circ$; the (1 0 2) peak shape was broad at about 273 K. The (1 1 0) peak was almost lost, and the (0 0 ℓ) peaks had strengthened at about 333 K, and new small peaks were observed at $2\theta = 39.5^\circ$ and 47.8°. In this study, we obtained tetragonal $PbSnF_4$, as reported in Ref. [11], through preparation at room temperature.

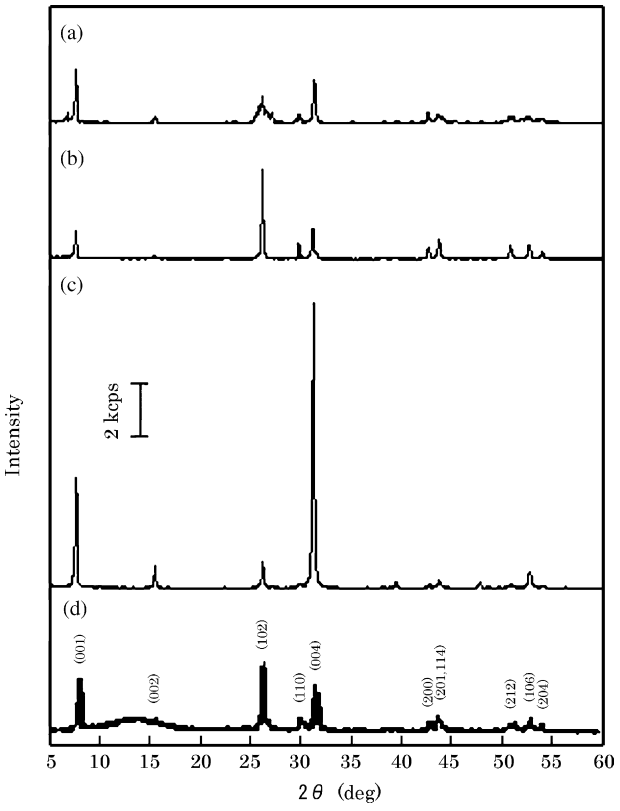

Fig. 1. XRD profiles of $PbSnF_4$ prepared at 273 K (a), 298 K (b) and 333 K (c), and reference (d).

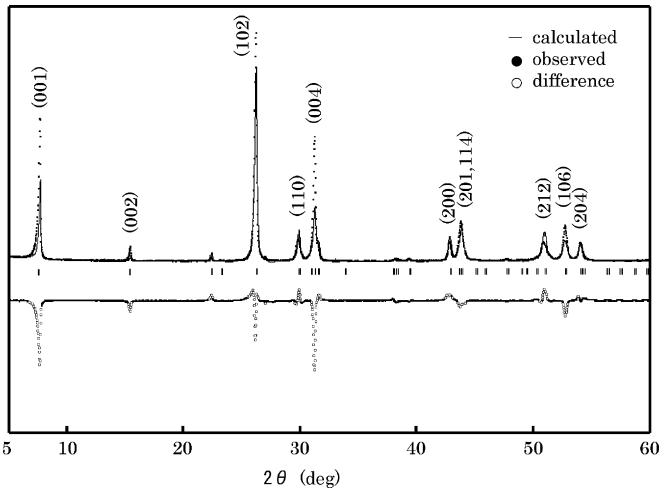

Fig. 2. Rietveld refinement profile of $PbSnF_4$ (−: calculated, ●: observed, ○: difference), $R_F = 7.09$, $S = 9.1397$.

Fig. 2 shows the profile of Rietveld refinement. The solid line in the profile was calculated using the RIETAN-2000 program [24]; the dotted line indicates data observed by XRD. The structure was determined in the tetragonal space group *P4/nmm*, with $a_0 = 0.4217$ nm, $c_0 = 1.1427$ nm; R_F was 7.09. This value was insufficiently small; some orthorhombic phase existed in the product.

A schematic illustration of the crystal lattice is shown in Fig. 3. Both Pb^{2+} and Sn^{2+} are ordered in the lattice. This ordering of Pb and Sn causes formation of vacancies of fluoride ion at the 4f and 8i site. Fluoride ions were transferred through these sites. Crystal parameters and interatomic distances are summarized in Tables 1 and 2. The theoretical density obtained from Rietveld refinement was 6.588 g cm^{-3} and the experimental density was 6.559 g cm^{-3}. The difference between the theoretical and experimental densities was 0.44%, which was considerably small.

On the other hand, the prepared sample was estimated, respectively, as $Pb_{1.2}SnF_{3.9}$, $PbSnF_{3.86–4.08}$ and $PbSnF_{3.8–4.12}$ using X-ray fluorescence spectroscopy (XFS), fluoride ion-selective electrode, and ion chromatography.

2.2. Electrochemical properties

Fig. 4 shows a Cole–Cole plot of tetragonal $PbSnF_4$ in air. It shows that a semi-circular arc with a tail at the low-frequency range is assignable to electrode interface effects. This type of Cole–Cole plot is analyzed using Randles' equivalent circuit [25–27]. The center of the semi-circle is located below the real axis, which might show the inductance component arise from an experimental problem. At first, the Randles' circuit was inferred to be an equivalent circuit consisting of double-layer capacitance, the charge transfer resistance, and Warburg impedance. However, it seemed that the circuit was more complicated here. In this study, a linear part in the Cole–Cole plot was extrapolated to the high-frequency side and the value was regarded as resistance of the sample because factors were not calculable. The value of the

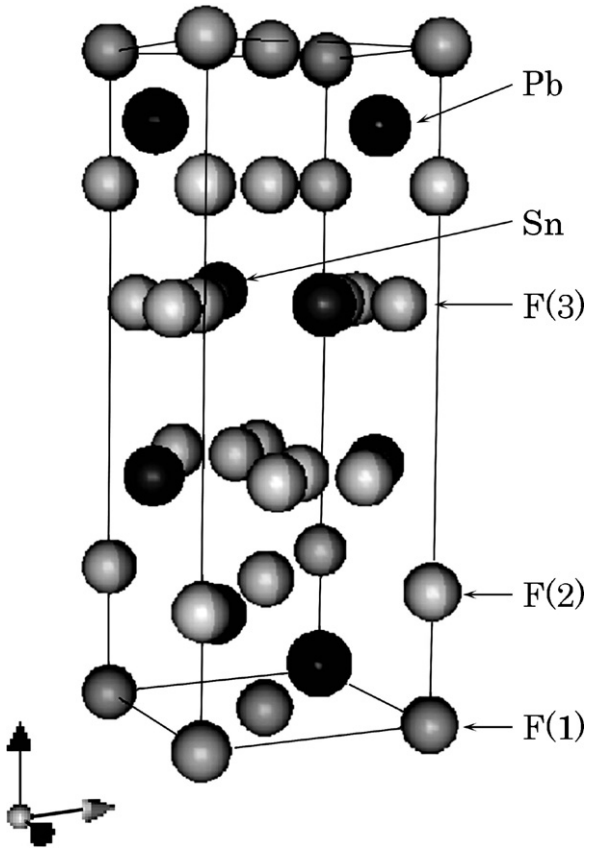

Fig. 3. Unit lattice of tetragonal $PbSnF_4$. $a_0 = 0.4217$ nm, $c_0 = 1.1427$ nm, space group *P4/nmm*.

extrapolated right crossing point of the impedance spectra to the real axis corresponding to dc resistance was about 65 Ω at 323 K. That is, dc conductivity was calculated as 0.54 Sm^{-1} at 323 K.

Table 1
Atomic parameter of Rietveld analysis of $PbSnF_4$

Atom	Site	*x*	*y*	*z*	Occupancy
Pb	2c	0	0.5	0.10995	1.0
Sn	2c	0	0.5	0.63036	1.0
F1	2a	0.5	0.5	0	1.0
F2	4f	0.5	0.5	0.2011	0.56
F3	8i	0	0.30901	0.37891	0.47

$V = 2.032 \times 10^{-28}$ m^{-3}, Dx = 6.588×10^{3} kg m^{-3}.

Table 2
Interatomic distance by Rietveld analysis of $PbSnF_4$

Bond	Length (nm)
Pb–F1	0.2454
Pb–F2	0.2351
Pb–F3	0.3177
Pb–Sn	0.4206
Sn–F1	0.4720
Sn–F2	0.2855
Sn–F3	0.2480
F1–F2	0.2297
F2–F3	0.2413
F3–F3	0.3324

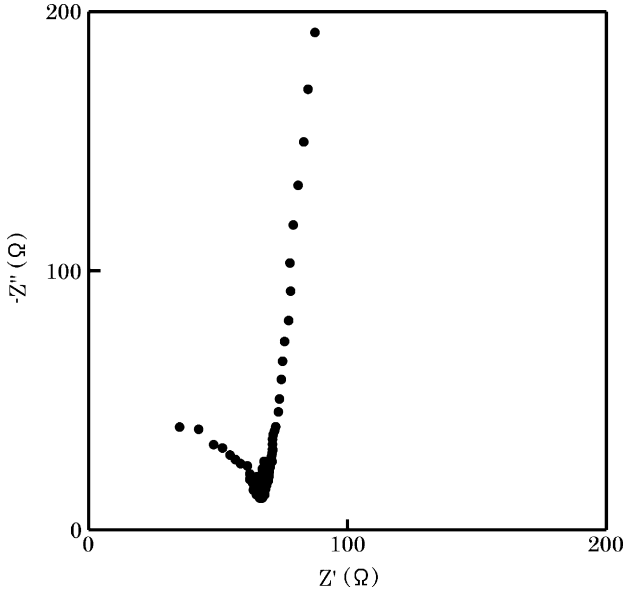

Fig. 4. Cole–Cole plot of tetragonal $PbSnF_4$ in air between 1 Hz and 500 kHz at 323 K. Sample thickness = 1 mm.

Fig. 5 shows Arrhenius plots of the electrical conductivity of tetragonal $PbSnF_4$ for temperatures of 286–473 K in various atmospheres.

A value higher than the reference value in the literature [11,13,22] was obtained in air and Ar. Tetragonal $PbSnF_4$ exhibited the highest conductivity of 3.2 Sm^{-1} at 473 K in air. The electric conductivity rose with increasing temperature; the Arrhenius plot showed a gradual slope change around 373 K from the high-temperature range to the low-temperature range in good agreement with the literatures. The activation energies were estimated as 25.0 kJ mol^{-1} at 373–286 K and 12.4 kJ mol^{-1} at 473–373 K.

The phase transitions in $PbSnF_4$ were already reported around 355 K [13,17,22]. It has been reported that the change in the slope of Arrhenius plots of tetragonal $PbSnF_4$ are found

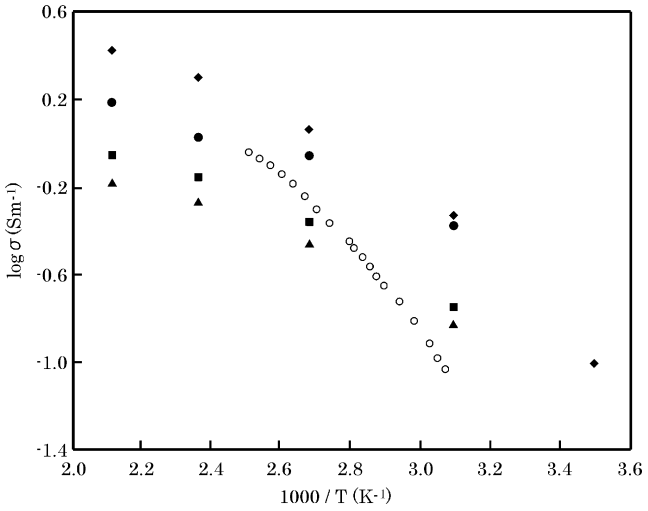

Fig. 5. Electrical conductivity of tetragonal $PbSnF_4$ upon cooling from 473 to 286 K. (a) In air (◆), (b) in vacuum (■), (c) in Ar (●) and in Ar flow (▲), and reference values (d) (○).

Table 3
Conductivities taken by electron and hole, σ_e and σ_h in $PbSnF_4$ at 423 and 373 K

Temperature (K)	Electron conductivity, σ_e (Sm^{-1})	Hole conductivity, σ_h (Sm^{-1})
423	4.4×10^{-5}	4.4×10^{-10}
373	9.5×10^{-6}	3.2×10^{-11}

around 355 K from the high-activation-energy region to the low-activation-energy region in the literatures [8,17,22,28].

Tetragonal $PbSnF_4$ might transform to the other phase, which has lower conductivity. Observed disagreements with values obtained from the literature might result from the different tetragonal $PbSnF_4$ concentration in the sample.

The ionic transport number of mobile species was estimated using Wagner's polarization method [29]. Fig. 6 shows the chronoamperogram of $PbSnF_4$ at 373 K. The current observed at 474 K was not sufficiently stable to carry out measurements. It increased gradually with elapsed time. The current was not well measured at 323 K either, because the current is so small in this case. At 423 K, the currents used at the steady state were 1.95 and 21.0 nA for applied voltages of 0.1 and 0.5 V, respectively. For 373 K, the currents were 0.38 and 8.13 nA for 0.1 and 0.5 V of the applied voltages, respectively. Results of chronoamperometry at 423 and 373 K are summarized in Table 3. The total current i includes both ionic and electronic currents. The electrons and holes contribute to the electronic current. The electron transport number (τ_e) was obtained using the following equation:

$$\frac{I}{\exp(u)-1} = \frac{RT[\sigma_h + \sigma_e \exp(-u)]}{FL}, \quad u = \frac{EF}{RT}$$

Therein, I is the current density, F the Faraday constant, approximately 96,500 coulombs per equivalent, L the thickness of the sample, E the applied voltage, σ_h is the hole conductivity, and σ_e is the electron conductivity. The electronic current was carried the electrons mainly because $\sigma_h \ll \sigma_e$. The electronic conductivities ($\sigma_h + \sigma_e \fallingdotseq \sigma_e$) were much smaller than the electrical conductivities of 1.52 and 1.13 Sm^{-1} (423 and 373 K), respectively. Therefore, the ionic transport number was found to be approximately 1. The tetragonal $PbSnF_4$ seems to be a good fluoride ion conductor.

2.3. Preparation of COF_2 in an electrochemical cell

We reported the reaction between CO_2 and F_2 to form COF_2 [4]. By that reaction, CO_2 is convertible to COF_2. The Gibbs free energy change of this reaction is calculated as $-220\ kJ\ mol^{-1}$ [5]. The theoretical electromotive force (emf) calculated from its Gibbs free energy is 1.14 V; that value is mostly equal to 1.23 V of the emf for the H_2/O_2 fuel cell [6]:

$$CO_2 + F_2 \rightarrow COF_2 + \tfrac{1}{2}O_2 + (-\Delta G)\ 220\ kJ\ mol^{-1}$$

A CO_2/F_2 electrochemical cell was constructed with a tetragonal $PbSnF_4$ disk having Au electrodes.

The reactions at anodes and cathodes are written as follows:

$$\text{Anode}: 2F^- \rightarrow F_2 + 2e, \qquad CO_2 + F_2 \rightarrow COF_2 + \tfrac{1}{2}O_2$$

$$\text{Cathode}: F_2 + 2e \rightarrow 2F^-$$

Therefore, $CO_2 + F_2 \rightarrow COF_2 + 1/2O_2$. As shown above, the tetragonal $PbSnF_4$ [7–21] is known as a fluoride ion conductor having high electric conductivity at ambient temperature. The CO_2/F_2 electrochemical cell was constructed using tetragonal $PbSnF_4$ with Au electrodes as the solid electrolyte; its performance was investigated using emf and impedance measurements.

Fig. 7 shows results of emf measurements under conditions of 0.1 MPa CO_2/(0.02 MPa F_2 + 0.08 MPa Ar) and 0.1 MPa CO_2/(0.01 MPa F_2 + 0.09 MPa Ar). The respective emf values were about 0.86 and 0.93 V at 0.02 MPa F_2 and 0.01 MPa F_2 in Ar. The measured emf value was about 80% of the theoretical one of 1.14 V. The difference between the emf value for 10–20% F_2 in Ar was calculated as 0.009 V. Commonly, the chemical potential becomes lower by the interfacial resistance of the electrolyte and the ectrode or the crossleak. Although some points require improvement, a CO_2/F_2 electrochemical cell can probably be constructed sufficiently with $PbSnF_4$ as a solid electrolyte. However, the measured short circuit current density was 0.24 A m^{-2}, which was quite small. It is important

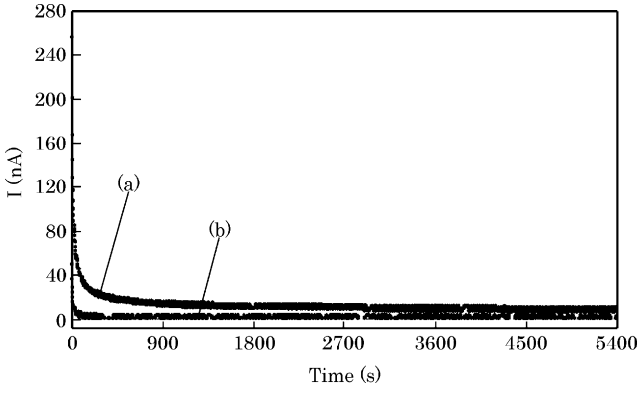

Fig. 6. Chronoamperometry for $PbSnF_4$ at 373 K. Applied p.d. = 0.5 V (a), 0.1 V (b). Sample thickness = 1 mm.

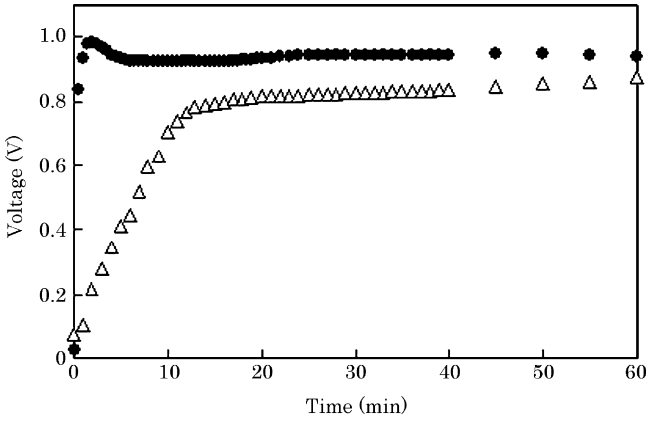

Fig. 7. The change in emf over time. Anode gas was 0.1 MPa CO_2 and cathode gas was χMPa F_2 + (0.1 − χ) MPa Ar. (●: χ = 0.01, △: χ = 0.02).

to mention here that the resistance, capacitance and impedance changed and became large by the effect of F_2 gas during the measurement. Apparently, the current value did not increase according to the effects of the morphological stability of electrode against F_2 gas. The electrolyte and the electrode interface might be very sensitive to F_2 gas, and the charge transfer process and mass transfer process might be affected by the exposure time of the sample under the F_2 environment.

The absorption peaks of fluorocarbon compound did not appear in the FT-IR spectra in which 1200–1300 cm^{-1} and around 1930 cm^{-1} corresponded to C–F and CF=O bonds, respectively. The current density was so small that the reaction between CO_2 and F_2 could not take place sufficiently and no fluorocarbon compound was detectable after 3 h discharge using FT-IR.

3. Conclusion

Tetragonal $PbSnF_4$, which had higher electrical conductivity than orthorhombic $PbSnF_4$, was prepared by adding $Pb(NO_3)_2$ aqueous solution to SnF_2 aqueous solution at dropping speed of 500 $mm^3\ s^{-1}$ at room temperature. The $PbSnF_4$ exhibited conductivity of 3.2 Sm^{-1} at 473 K in air.

A CO_2/F_2 electrochemical cell was constructed using tetragonal $PbSnF_4$ with Au electrodes as the solid electrolyte. The electromotive force was about 0.9 V at room temperature under conditions of 0.1 MPa CO_2/(0.01 MPa F_2 + 0.09 MPa Ar). The short circuit current density was measured as 0.24 A m^{-2}.

The content of the fluorocarbon compound as the product was so low that it could not be detected.

4. Experimental

4.1. Preparation of $PbSnF_4$

$PbSnF_4$ was prepared by adding a 1.01 M aqueous solution of $Pb(NO_3)_2$ (99.5%) to a freshly prepared 2.47 M aqueous solution of SnF_2 (99%) with the ratio of Pb/Sn = 0.25:

$$Pb(NO_3)_2 + 4SnF_2 \rightarrow PbSnF_4 + Sn(NO_3)_2 + 2SnF_2$$

The white sediment prepared by dropping $Pb(NO_3)_2$ aqueous solution to SnF_2 aqueous solution was suction-filtered and placed in vacuum (ca. 10^{-2} mm of Hg) for at least 4 h.

4.2. Characterization of $PbSnF_4$

The sample was characterized using X-ray diffraction (XRD) and analyzed by energy dispersive X-ray fluorescence spectrometry (XFS), density measurement, and quantitative analysis of fluoride ion.

Using XFS (EDX-800; Shimadzu Corp.), a calibration curve was plotted for quantitative analysis of samples. The molar ratios of PbF_2 and SnF_2 in pellets as standard samples were adjusted to 1:0, 1:4, 2:3, 3:2, 4:1, and 0:1. Density was measured (Micrometics Accupyc 1330; Shimadzu Corp.).

A fluoride-ion-selective electrode (SA720; Orion Research Inc.) and ion chromatography (Tosoh Corp.) were used for quantitative analyses of fluoride ions.

The spacing of atoms in a solid can be measured using X-rays. X-ray diffraction data were collected using a diffractometer (XD-3As; Shimadzu Corp.) with Cu Kα radiation (1.5418 Å). Data were collected at a scan rate of 2°/min by sampling pitch 0.034°, with a preset time of 4 s. Rietveld analyses of the X-ray power diffraction pattern were carried out. The crystal structure parameters were refined using Rietveld analysis with the RIETAN-2000 program [24].

The sample of about 1 g was compacted into a pelleter. After vacuuming for 15 min, the sample was pelletized to 13 mm $\varphi \times 1$ mm under the condition of 4.5 MPa for 5 min. Gold electrodes were vapor-deposited with cross-sectional area of 28.3 mm^2 on both surfaces of the $PbSnF_4$ pellet using an ion coater (IC-50; Shimadzu Corp.).

The pellet was set in a cell assembly that was designed specially to measure the electrical conductivity, as shown in Fig. 8; the pellet was sandwiched and pressed between two Pt electrodes. The electrical conductivity was measured using ac impedance method (Frequency Response Detector Model 1025, Potentiostat/Galvanostat Model 273A; EG & G Instruments). This measurement was done for frequencies of 500 kHz and 1 Hz. Temperature variations of ac conductivities were

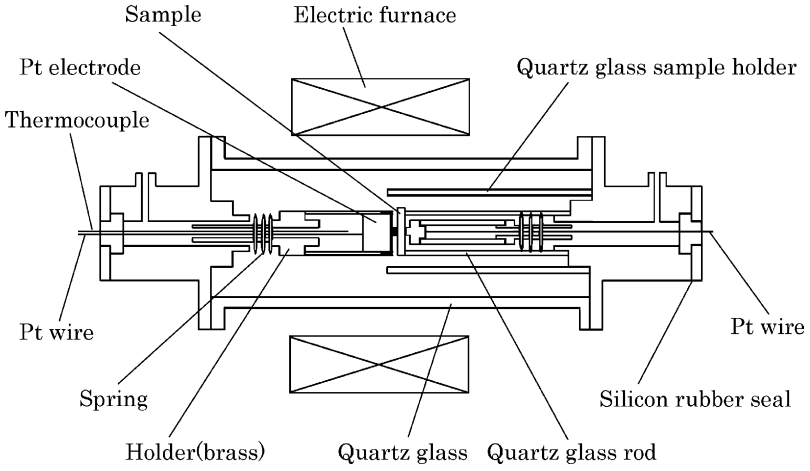

Fig. 8. Schematic illustration of the original designed cell.

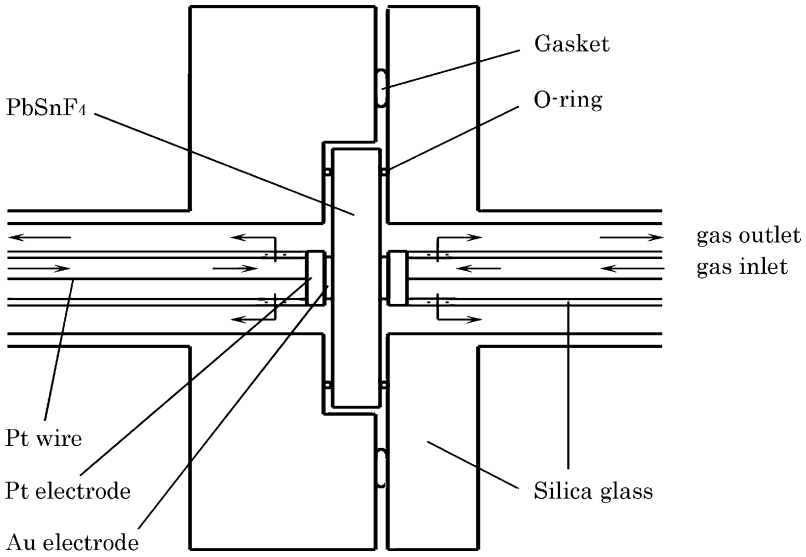

Fig. 9. Schematic diagram of the CO_2/F_2 electrochemical cell.

recorded for temperatures of 286–473 K. The polarization current was recorded as a function of time and was recorded using a computerized data acquisition system. The ac conductivities depicted the Arrhenius behavior of $PbSnF_4$ using a temperature variation setup.

The ion transport number of the sample was estimated using Wagner's dc polarization method [29]. Before dc polarization measurement, the electrical conductivity of the sample in argon was measured. After heating to an appropriate temperature, voltage was applied and the leak current was measured using chronoamperometry (Potentiostat/Galvanostat Model 273A; EG & G Instruments) using the same setup. The steady volt-ampere characteristics of the specimen were also measured. Partial electron hole and electronic conductivities were obtained. Then, the electronic transport number was calculated.

4.3. Preparation of COF_2

Fig. 9 is an image of a CO_2/F_2 electrochemical cell. It is expected that the electrochemical cell would be applied at a low temperature by our research.

A CO_2/F_2 electrochemical cell was constructed using a reactive line and an original cell for electromotive force measurement. A $PbSnF_4$ disk was prepared for the electromotive force measurement. A sample of about 2.5 g was compacted into a pelleter. After vacuuming for 15 min, the sample was pelletized

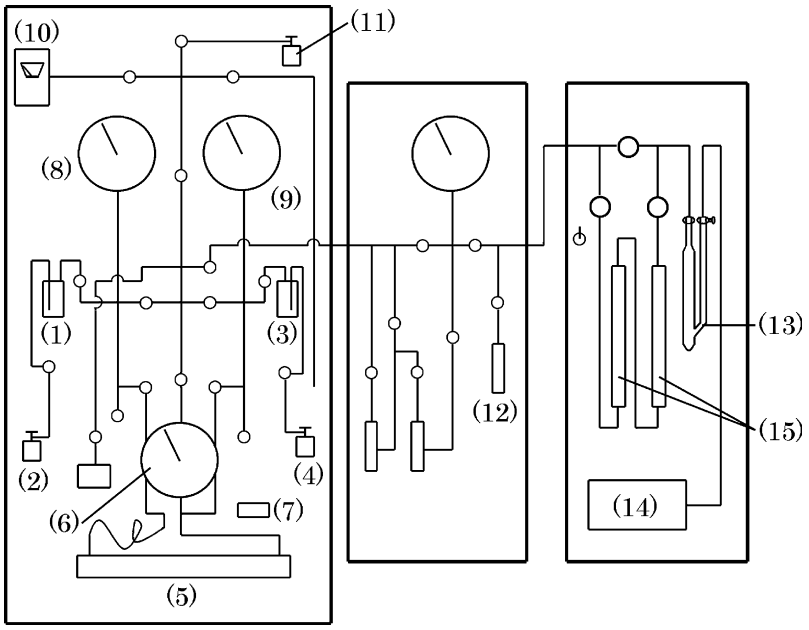

Fig. 10. Schematic diagram of original line for electromotive force measurement. (1) CO_2 gas storage, (2) CO_2 gas cylinder, (3) F_2 gas storage, (4) F_2 gas cylinder, (5) cell for electromotive force, (6) F_2 gas pressure gauge, (7) F_2 gas pressure digital gauge, (8) CO_2 gas pressure gauge, (9) F_2 gas pressure gauge, (10) PIRANI gauge, (11) Ar gas cylinder, (12) gas sampler, (13) trap (liq. N_2), (14) vacuum pump (oil rotary), (15) activated alumina.

to 20 mm $\varphi \times 1.2$ mm under 9.5 MPa for 5 min. The relative density of the pellet of the $PbSnF_4$ prepared here was about 0.87.

The pellet was polished and a porous Au electrode was vapor-deposited onto the $PbSnF_4$ pellet surface. Fig. 9 shows that the pellet was set in a cell assembly designed specially to measure the electromotive force. In addition, the cell was connected to an original line, as shown in Fig. 10.

The CO_2 and F_2 in Ar, argon balance, were put in the cell, respectively, in 0.1 MPa and the electromotive force was measured. That arrangement produced a closed circuit and the current was measured when the electromotive force was steady.

The CO_2 gas of the anode side was put in an IR cell after the current had been measured in the closed circuit for 3 h at 373 K. The gaseous product at the anode was analyzed using FT-IR spectroscopy.

References

[1] I. Omae, Nisankatannso to Tikyukankyou, Tyukousinnsho (1999) 23–142. http://cdiac.esd.ornl.gov/trens/emis/em_cont.htm.
[2] Y. Matsumoto, M. Obata, J. Hombo, J. Phys. Chem. 98 (1994) 2950–2951.
[3] W.M. Sears, S.R. Morrison, J. Phys. Chem. 89 (1985) 3295–3298.
[4] Y. Hasegawa, R. Otani, S. Yonezawa, M. Takashima, J. Fluorine Chem. 128 (2007) 17–28.
[5] J.C. Amphlett, J.R. Dacey, G.O. Pritchard, J. Phys. Chem. 75 (1971) 3024–3026.
[6] W.M. Latimer, The Oxidation States of the Elements and their Potentials in Aqueous Solutions, Prentice Hall, New York, 1952.
[7] D.J. Donaldson, B.J. Senior, J. Chem. Soc. (A) (1967) 1821–1825.
[8] J.M. Reau, C. Lucat, J. Portior, P. Hagenmuller, L. Cot, S. Vilminot, Mater. Res. Bull. 13 (1978) 877–882.
[9] J. Pannetier, G. Denes, J. Lucas, Mater. Res. Bull. 14 (1979) 627–631.
[10] G. Perez, S. Vimont, W. Granier, L. Cot, C. Lucat, J.M. Reau, J. Portior, P. Hagenmuller, Mater. Res. Bull. 15 (1980) 587–593.
[11] G. Denes, M.C. Madamda, A. Muntasar, A. Peroutka, K. Tam, Z. Zhu, Nato, Sci. Ser. (1999) 25–38.
[12] G. Denes, J. Solid State Chem. 77 (1988) 54–59.
[13] G. Denes, T. Birchall, M. Sayer, M.F. Bell, Solid State Ionics 13 (1988) 213–219.
[14] Y. Ito, T. Mukuyama, H. Funatomi, S. Yoshikado, T. Tanaka, Solid State Ionics 67 (1994) 301–305.
[15] R. Kanno, K. Ohno, H. Izumi, T. Kamiyama, H. Asamo, F. Izumi, Y. Solid State Ionics 70–71 (1994) 253–258.
[16] G. Denes, Y.H. Yu, T. Tyliszczak, A.P. Hitchcock, J. Solid State Chem. 91 (1991) 1–15.
[17] M.M. Ahmad, K. Yamada, T. Okuda, J. Phys. Condens. Matter 14 (2002) 7233–7244.
[18] S. Suda, T. Eguchi, J. Kuwano, Key Eng. Mater. 181–182 (2000) 203–206.
[19] A. Wakagi, J. Kuwano, Y. Saito, J. Mater. Chem. 41 (1994) 973–975.
[20] T. Eguti, S. Suda, T. Hijii, S. Koga, J. Kuwano, Y. Saito, Key Eng. Mater. 181–182 (2000) 199–202.
[21] A. Wakagi, J. Kuwano, M. Kato, H. Hanamoto, Solid State Ionics 70–71 (1991) 601–605.
[22] G. Denes, G. Milova, M.C. Madamda, M. Perfiliev, Solid State Ionics 86–88 (1996) 77–82.
[23] Joint Committee for Powder Diffraction Standards (JCPDS), International Centre For Diffraction Data.
[24] F. Izumi, T. Ikeda, Mater. Sci. Forum 321–324 (2000) 198–203.
[25] J.E.B. Randles, Discuss. Faraday Soc. 1 (1947) 11–19.
[26] J.E.B. Randles, Trans. Faraday Soc. 44 (1948) 327–338.
[27] J.E.B. Randles, Trans. Faraday Soc. 52 (1956) 1573–1581.
[28] R. Kanno, S. Nakamura, K. Ohno, Y. Kawamoto, Mater. Res. Bull. 26 (1991) 1111–1117.
[29] J.B. Wagner, J.C. Wagner, J. Chem. Phys. 26 (1957) 1597–1601.